Journal of Hazardous Materials 217–218 (2012) 29–35

Contents lists available at SciVerse ScienceDirect

Journal of Hazardous Materials

journal homepage: www.elsevier.com/locate/jhazmat

# Removal of phosphorus by a composite metal oxide adsorbent derived from manganese ore tailings

Ting Liu[a,b,*], Kun Wu[c], Lihua Zeng[a]

[a] College of Resources and Environment, Northwest A & F University, Yangling, Shaanxi 712100, China
[b] Key Laboratory of Plant Nutrition and the Agri-environment in Northwest China, Ministry of Agriculture, Yangling, Shaanxi 712100, China
[c] School of Environmental and Municipal Engineering, Xi'an University of Architecture and Technology, Xi'an, Shaanxi 710055, China

ARTICLE INFO

*Article history:*
Received 10 October 2011
Received in revised form
25 December 2011
Accepted 4 January 2012
Available online 9 March 2012

*Keywords:*
Phosphate
Adsorption
Composite metal oxides
Manganese ore tailings

ABSTRACT

The selective adsorption of phosphate (P) from wastewater is a promising method for controlling eutrophication in water bodies. In this study, an adsorbent of composite metal oxides (CMOMO) was synthesized from manganese ore tailings by the process of digestion–oxidation–coprecipitation. CMOMO was characterized using several methods, and its adsorption behaviors for phosphate were investigated. Based on the results from SEM and BET analysis, CMOMO exhibited a rough surface and a large surface area (307.21 $m^2/g$). According to the results of EDAX, XRD and XPS, its main constituents were determined to be amorphous FeOOH, $MnO_2$ and AlOOH. The kinetic data were best fit using the Elovich model due to its complicate composites. The maximal adsorption capacity of P would increase with elevated temperatures. Additionally, it was found that the P removal efficiency decreased with an increase of pH (4–10) or a decrease of ion strength (1–0.01 M). The coexisting anions had little effects on phosphate removal, implying the specific adsorption of P by CMOMO. Furthermore, the desorption and reuse results indicated that this adsorbent could be regenerated using alkali solutions.

© 2012 Elsevier B.V. All rights reserved.

## 1. Introduction

The enhanced removal of phosphate (P) from wastewater may become required urgently when it is discharged to freshwater bodies, which are at a risk of eutrophication [1]. Several methods have been developed for P removal, such as chemical precipitation [2], biological processes [3,4], adsorption [5], ion exchange [6], and membrane technologies [7]. Among these available approaches, chemical precipitation and biological processes are generally not able to meet the stringent effluent standards, while ion exchange and membrane technologies need high investment and operation cost. Comparing with these methods, adsorption process showed advantages of easily-handle operation, high efficiency and lower cost. Various adsorbents have been used for P removal, such as zeolite [8], Ca-based materials [9], iron oxides [10], aluminum oxides [11], etc. In recent years, based on economical and environmental concerns, considerable attention has been paid to the utilization of low-cost adsorbents, including agro-industrial and municipal waste materials [12]. Some of these waste materials were used directly for P removal from wastewater. Razali et al. [13] studied the effectiveness of drinking water treatment sludge in removing different phosphorus species from aqueous solution, and found the Al-based sludge had the potential to be used as a raw material for a wide range of P species removal in simulated P-enriched wastewater. Wei et al. [14] used acid drainage sludge for the P removal from secondary effluents of municipal wastewater treatment plants. It was found that the metal oxides (such as iron (Fe), aluminum (Al), manganese (Mn), etc.) contained in these low-cost adsorbents played an important role for their capacity for phosphate removal [14]. However, the adsorption capacities of these waste materials were generally limited due to the less active components [13,14]. Moreover, second pollution may be caused due to the complicate components of these materials. Thus, some researchers have made efforts to effectively utilize these waste materials for the preparation of adsorbents with low cost and high adsorption capacity. Gong et al. [15] prepared a new adsorbent with hydrated lime and blast furnace slag for phosphorus removal from aqueous solution, and optimized the preparation conditions for the premium P removal efficiency. Sibrell et al. [16] prepared an adsorption media from acid mine drainage sludge for the P removal from agricultural wastewater, which was more safe and had a greater P adsorption capacity than that of acid mine drainage sludge.

Manganese ore tailings were produced hundreds of thousands of tons every year in China, due to the exploitation of manganese ores. It has been reported that the metals contained in the wastes of abandoned mines may cause serious environmental problems in

* Corresponding author at: College of Resources and Environment, Northwest A & F University, Yangling, Shaanxi 712100, China. Tel.: +86 29 87082317; fax: +86 29 87080065.
*E-mail addresses:* liuting8206@yahoo.cn, tomlucy2005@yahoo.cn (T. Liu).

0304-3894/$ – see front matter © 2012 Elsevier B.V. All rights reserved.
doi:10.1016/j.jhazmat.2012.01.019

**Table 1**
Analytical results of certified metal materials in manganese ore tailings.

| Metal components | Mass percentage (%) |
|---|---|
| Mn | 10.72 ± 2.52 |
| Fe | 7.70 ± 1.53 |
| Al | 1.57 ± 0.19 |
| Ca | 1.51 ± 0.35 |
| Mg | 1.14 ± 0.36 |
| K | 0.81 ± 0.11 |
| Ni | 1.48 ± 0.24 |
| Nb | 3.24 ± 0.31 |

nearby groundwater, stream and cultivated lands [17,18]. So these mine wastes should be disposed of properly to minimize the threat for the ecology environment. A mineralogical study showed that this mine waste is composed primarily of Mn, Fe and silicon (Si) oxides (pyrolusite, hematite, quartz, . . .) [19]. It may be beneficial to synthesize a material of composite metal oxides from manganese ore tailings and use it as an adsorbent for removing phosphate, which provides not only an effective residual management option for manganese ore tailings, but also an alternative approach for P removal.

Therefore, the objective of this study was to explore the feasibility of the composite mental oxides derived from manganese ore tailings (CMOMO) for P removal. The surface characteristics research of CMOMO was conducted. The kinetics and isotherm behaviors of phosphate adsorption by CMOMO were investigated. The parameters influencing P removal were also studied, including solution pH and coexisting anions. Additionally, the P desorption from CMOMO was performed to assess the regeneration feasibility.

## 2. Experimental

### 2.1. Materials

The mine tailings used in this study were gotten from a mine of manganese ores at the city of Hanzhong in Shaanxi Province, China. The metal compositions were shown in Table 1.

All chemicals were of analytical grade and purchased from Beijing Chemical Co., and all solutions were prepared with deionized water. Sodium hypochlorite (NaClO) was used for the preparation the adsorbent. The phosphorus stock solutions were prepared with sodium dihydrogen phosphate ($NaH_2PO_4$). Additionally, sodium nitrate ($NaNO_3$) was used to fix a constant ion strength (0.01 M $NaNO_3$) of solutions. Additionally, sodium hydroxide (NaOH) and hydrochloric acid (HCl) were used to adjust pH of solutions.

### 2.2. Preparation of adsorbent

The process to prepare the adsorbent from manganese ores (CMOMO) was similar with the method of $MnO_2$ preparation from Moroccan pyrolusite mine waste [20]. Firstly, manganese ore tailings were crushed and sieved below the particle size of 0.125 mm, and then put into HCl solution (6 mol/L) in a flask with the solid/liquid ratio of 90 g/L, mixing at a temperature of 323 K for 12 h. Secondly, the solution was filtered to separate the silica content, and the filtrate was conditioned at pH = 6 with NaOH solution (5 M). After that, the resulting solution was oxidized completely by hypochlorite ion ($ClO^-$), and the solution pH was maintained in the range of 6–8 using HCl and NaOH solutions. Finally, the precipitates were sampled, washed with distilled water, dried at 378 K for 6 h, crushed and stored for use.

### 2.3. Batch adsorption experiments

All experiments were conducted at (298 ± 1 K) on a mechanical orbit shaker at 130 rpm for 24 h. For kinetics experimental study, 0.5 g CMOMO was added into 1000 mL of 5 mg/L or 15 mg/L phosphate solution with an ionic strength of 0.01 M $NaNO_3$ at pH 6.0. The samples were taken at different time intervals and filtered with a 0.45 μm polycarbonate filter membrane.

In the sorption isotherm study, 0.05 g CMOMO was added into 100 mL of phosphate solution with different initial concentrations from 5 mg/L to 60 mg/L and a same ionic strength of 0.01 M $NaNO_3$ at pH 6.0. Samples were taken after 24 h of contact and filtered with a 0.45 μm polycarbonate filter membrane.

In order to test the effects of pH and ion strength, 100 mL of 5 mg/L phosphate solutions with varied concentrations of $NaNO_3$ (0.01–1 M) at various initial pH (4.0–10.0) were prepared in 150 mL conical flasks. The solutions were measured and adjusted accordingly during the experiments by 0.1 M HCl and 0.1 M NaOH.

In the coexisting anions effect experiment, 100 mL of 5 mg/L phosphate solutions with 4 different anions (chloride ion, carbonate, silicate and sulfate) were prepared in conical flasks. For competitive adsorption of phosphate vs. these coexisting anions, a series of molar ratios of phosphate to chloride/sulfate/silicate/carbonate (5:1, 1:1, and 1:5) were employed, and the solution pH and ionic strength were controlled at 6.0 and 0.01 M $NaNO_3$. Other procedures were the same as those in the above isotherm experiments.

### 2.4. Analytical methods and characterizations

Total phosphorus (P(tot)) concentrations were determined using an ICP-OES (SCIEX Perkin Elmer Elan mode 5000, U.S.A.). Prior to analysis, the aqueous samples were acidified with $HNO_3$ in an amount of 1%, and stored in acid-washed glassware vessels.

The surface area was measured by the BET method using the Micrometritics ASAP 2000 surface area analyzer (U.S.A.). The samples were analyzed using a scanning electron microscope (SEM) with an EDAX KEVEX level 4 (Hitachi S-3500N, Japan). Before the analysis, the samples were sputtering coated (Quorum Polaron SC7620 Mini-sputter Coater) with gold/palladium (45 s) in order to reduce the charging effect in the microscope. An acid digestion method [21] was applied to measure amounts of metal elements in manganese ore tailings. X-ray diffraction analysis was carried out on a D/Max-3A diffractometer (Japan) using Ni-filtered copper Kα1 radiation. The treated samples were grounded to a fine powder using a mortar and pestle before analysis. The samples for zeta-potential analysis were investigated without filtration at room temperature with a Zetasizer 3000HSA (Malvern Instruments Ltd, UK). X-ray photoelectron spectroscopy (XPS) data were collected on an ESCA-lab-220i-XL spectrometer (Shimadzu, Japan) with monochromatic Al Kα radiation (1486.4 eV).

### 2.5. Desorption and reuse studies

To evaluate phosphate desorption from the CMOMO, the residual solids retained on the filter membrane were collected and dried after the filtration of the suspension from adsorption tests. 0.05 g phosphate-loaded CMOMO was added into each 150 mL flask containing 100 mL solution with different concentrations of NaOH (0, 0.001, 0.01, 0.1, and 0.5 M). $NaNO_3$ was added to adjust the ionic strength of the solution to 0.01 M. The flask was then shaken at 130 rpm for 24 h at 298 ± 1 K. The suspension solution was filtered and analyzed for desorbed phosphate in a similar way as described previously. The amount of desorbed phosphate was determined as the ratio of the desorbed P over the total P adsorbed by the

adsorbent. After the regeneration process, the samples were collected, washed with deionized water and freeze-dried for reuse.

### 2.6. Theory

In order to investigate the potential rate-controlling step of the P adsorption process, the kinetics data were fitted to the five models, which were respectively presented as follows in Eqs. (1)–(5) [22–25]:

$$q_t = q_e(1 - e^{-k_1 t}) \quad \text{pseudo-first-order model} \tag{1}$$

$$\frac{t}{q} = \frac{t}{q_e} + \frac{1}{k_2 q_e^2} \quad \text{pseudo-second-order model} \tag{2}$$

$$q_t = \frac{1}{\beta}\ln\ t + \frac{1}{\beta}\ln(\alpha\beta) \quad \text{Elovich model} \tag{3}$$

$$\ln\ q_t = \ln(kq_e) + \frac{1}{m}\ln t \quad \text{Power model} \tag{4}$$

$$q_t = k_{id}t^{0.5} + C \quad \text{intra-particle diffusion model} \tag{5}$$

where $t$ is the contact time of adsorption experiment (h); $q_e$ (mg/g) and $q_t$ (mg/g) are respectively the adsorption capacity at equilibrium and at any time $t$; $k_1$ (1/h), $k_2$ (g/mg h), $\alpha$ (mg/g h), $\beta$ (g/mg), $k$, $m$ and $k_{id}$ (mg/g $h^{0.5}$) are the rate constants for these models, respectively. Based on the $R^2$ results, the kinetics of phosphate adsorption on CMOMO can be satisfactorily described by either Power model or Elovich model.

To provide quantitative information for isotherms, these data were respectively fitted by Langmuir and Freundlich isotherm models [26,27]:

$$q_e = K_F C_e^{1/n} \quad \text{Freundlich model} \tag{6}$$

$$q_e = \frac{q_m b C_e}{1 + bC_e} \quad \text{Langmuir model} \tag{7}$$

where $C_e$ is the P concentration in the solution (mg/L), $q_e$ is the P concentrations in the solid adsorbent (mg/g), $q_m$ is the maximum adsorption capacity (mg/g), $K_F$ is a constant related to the adsorption capacity (mg$^{1-1/n}$ L$^{1/n}$/g), $b$ is a constant related to the energy of adsorption (L/g), $n$ is a constant related to the energy of adsorption.

To further evaluate the thermodynamic feasibility of the process and to study the nature of the adsorption process, the thermodynamic constants, standard free energy change ($\Delta G$), enthalpy change ($\Delta H$), and entropy change ($\Delta S$) were calculated using the following equations [28],

$$\Delta G = \Delta H - T\ \Delta S \tag{8}$$

$$\ln K = -\frac{\Delta H}{RT} + \frac{\Delta S}{R} \tag{9}$$

where $T$ (K) is the temperature, $R$ is an universal gas constant (8.314 J/mol K), and $K$ is the equilibrium constant related to the Langmuir constant ($b$) which can be determined according to following equation,

$$K = b \times 55.5 \tag{10}$$

where the value of 55.5 corresponds to the molar concentration of the solvent (water) [29].

## 3. Results and discussion

### 3.1. Characterizations

Fig. 1 presents the morphology and surface elements distribution of the CMOMO examined by SEM/EDAX. It can be seen that the adsorbent particles were aggregated with many small particles (Fig. 1a), resulting in a rough surface and a porous structure.

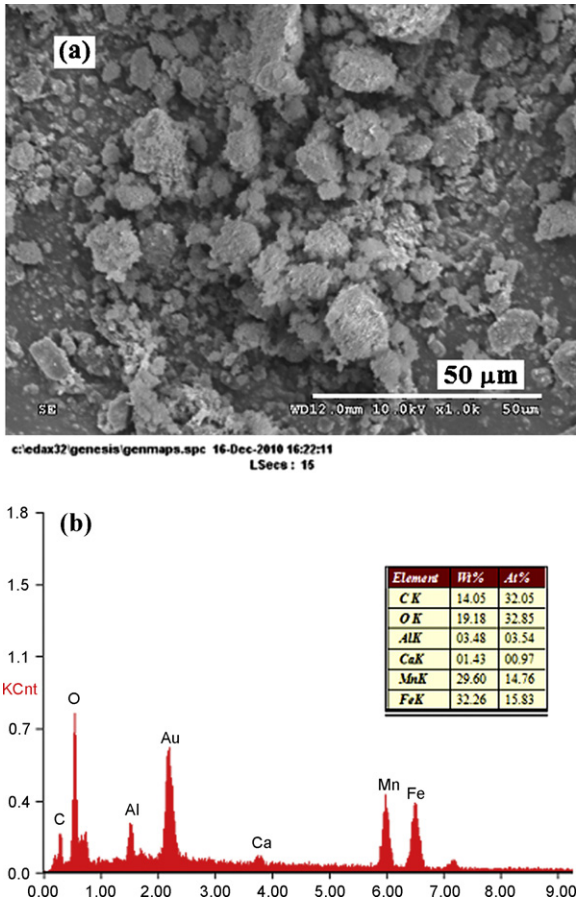


**Fig. 1.** SEM-EDAX results of CMOMO.

EDAX results showed that the adsorbent mainly contained the elements of O, Fe, Mn, Al and Ca, indicating the composition of mixed metal oxides. Chemical composition analysis revealed that Fe and Mn oxides were the dominant components of the adsorbent. In addition, the material had a high BET specific surface area of 307.21 $m^2$/g.

X-ray diffraction pattern of prepared CMOMO is illustrated in Fig. 2. The adsorbent showed an amorphous pattern with a peak present at 37.3°, which is typical of the synthetic birnessite phase δ-$MnO_2$ [30].

As both the element of Fe and Mn commonly have various valence states (mainly Fe(II) & Fe(III), Mn(II) & Mn(IV)), XPS analysis tests were performed to investigate the species distribution of Fe

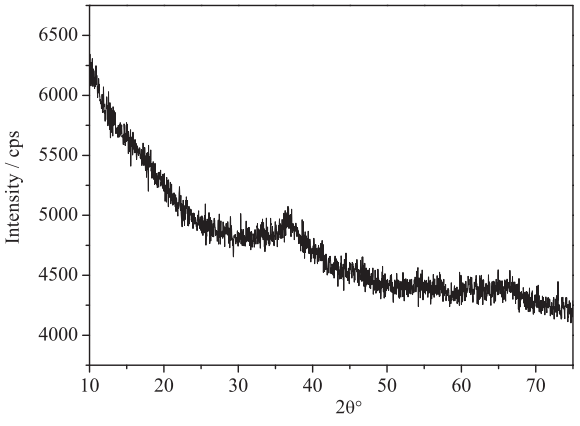


**Fig. 2.** XRD spectra of CMOMO.

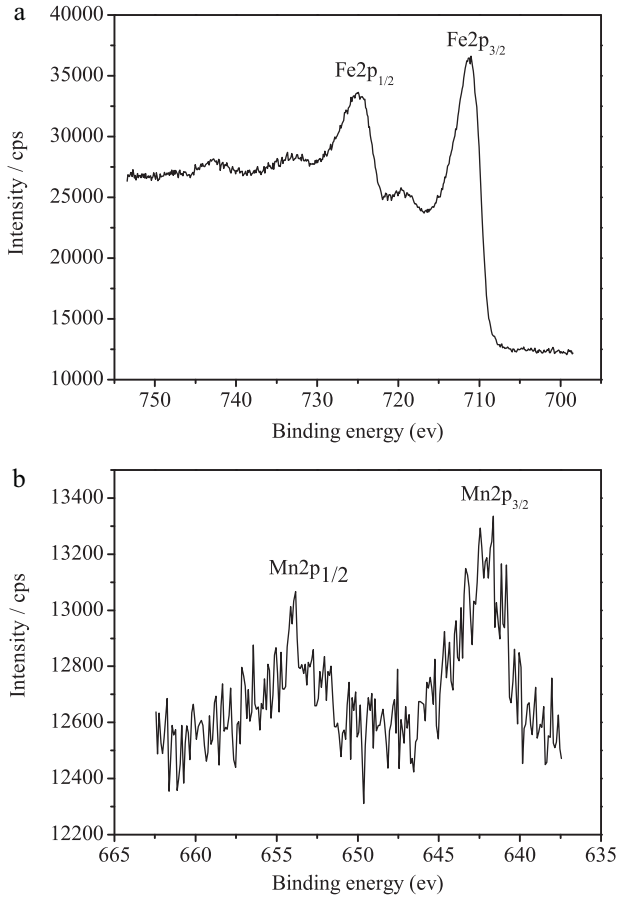


**Fig. 3.** XPS spectra of CMOMO: (a) Fe2p, and (b) Mn2p.

and Mn oxides in CMOMO. It is shown in Fig. 3 that the XPS spectra of $Fe2p_{1/2}$ & $Fe2p_{3/2}$ and $Mn2p_{1/2}$ & $Mn2p_{3/2}$ within CMOMO had the binding energies of 724.9 eV & 711.04 eV and 653.9 eV & 641.9 eV, respectively. $Fe2p_{3/2}$ binding energies of 711.0–711.6 eV were reported to be characteristic of Fe(III) species [31], inferring that Fe(III) dominated the oxidation state of Fe oxide within CMOMO. According to the research of Nesbitt et al. [32], the species of Mn oxide was determined to be Mn(IV). Thus, Fe and Mn in the synthesized adsorbent were in the oxidation states +(III) and +(IV), respectively. It could be concluded that CMOMO was mainly comprised with amorphous Fe(III), Mn(IV) and Al(III) oxides.

### 3.2. Kinetics

Fig. 4 shows the adsorption kinetics of P onto CMOMO at two different initial P concentrations. It can be seen that a large proportion of P was adsorbed in the first 3 h. The prolonged contact time of 21 h increased the adsorption capacity ($q_t$) values of P by 11.1% and 24.1% at the initial P concentrations of 5 mg/L and 15 mg/L, respectively. The adsorption process could be divided into two distinctive sections ($t < 3$ h and $t > 3$ h), which was confirmed by Fig. S1. It is indicted that the adsorption process was a chemisorption one, which was reported to be composed of two stages, fast and slow [33,34]. Comparing with other P removal adsorbents, such as goethite [35], the fast adsorption stage in our study was relatively longer, suggesting a slower penetration of the adsorbate into the adsorbent. It was reported [36] that the most important factors determining a slow penetration in the adsorption system are the high heterogeneity of the adsorbent and the strong non-ideality of

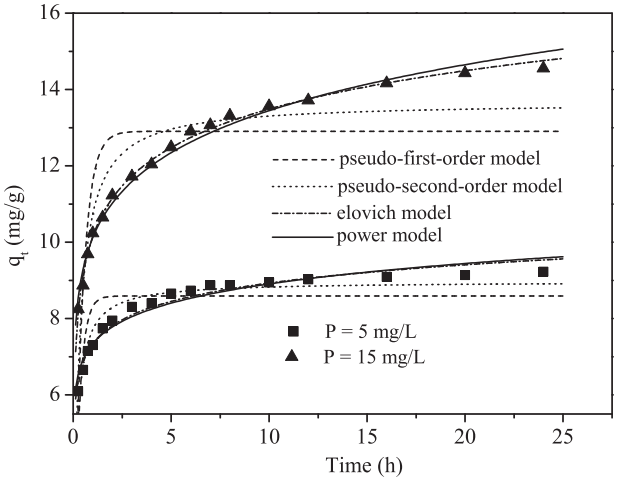


**Fig. 4.** Kinetics of P adsorption by CMOMO. Symbols indicate experimental data; dash lines represent the pseudo-first-order model; dot lines refer to the pseudo-second-order model; dash dot lines refer to the Elovich model; solid lines refer to the Power model (experimental conditions: initial P = 5 mg/L or 15 mg/L, pH = 6.0 ± 0.1, adsorbent dosage = 0.5 g/L).

the adsorbate. Thus, the slow penetration of P could be attributed to the high heterogeneity of CMOMO.

Table S1 presents parameters of 3 kinetics models for the P adsorption onto CMOMO. This high applicability of the Elovich model for the present kinetic data is generally in agreement with previous studies about the phosphate adsorption on soil minerals and iron oxide tailings [37,38]. This model has been proven to be suitable for highly heterogeneous systems—the common point of these adsorbents. Due to the composite constituents, CMOMO might exhibit different activation energies for chemisorption on the surface. Additionally, the decrease of $\alpha$ value with the increase of initial P concentrations suggested the more favorable adsorption of P at low concentrations. On the other side, the fitting of Power model was also rather good, which came to the similar results with previous studies [38]. Rudzinski et al. [36] stated that Power model is likely to be valid in the case of moderately heterogeneous surfaces, and proposed that there might be a hybrid between Elovich model and Power model, leading the satisfactory correlation of kinetics data with both of them.

### 3.3. Isotherm

Fig. 5 illustrates the adsorption capacities of P onto CMOMO at various temperatures. It is clear that the elevated temperatures favored the P adsorption by CMOMO. Adsorption isotherm provides an insight on the adsorptive performances of different adsorbents towards phosphate.

Table S2 illustrates the parameters of Langmuir and Freundlich isotherms for the P adsorption onto CMOMO. The $R^2$ values indicated that the Freundlich model fitted the data better than the Langmuir model. This can be also attributed to the heterogeneity of the adsorbent surface, because the Freundlich isotherm describes the adsorption by the adsorbent which has a heterogeneous surface with adsorption sites that have different energies of adsorption. Compared to most of the other low-cost adsorbents, CMOMO exhibited a greater capacity for P adsorption at ambient temperatures (Table 2). In addition, the increasing values of $q_m$ or $K_F$ with temperatures increasing inferred that the adsorption process was endothermic in nature.

It was found that the $\Delta G$ value decreased from −7.93 to −9.34 kJ/mol when the temperature varied from 298 to 318 K in this study, inferring the increase in spontaneity of the reactions. The

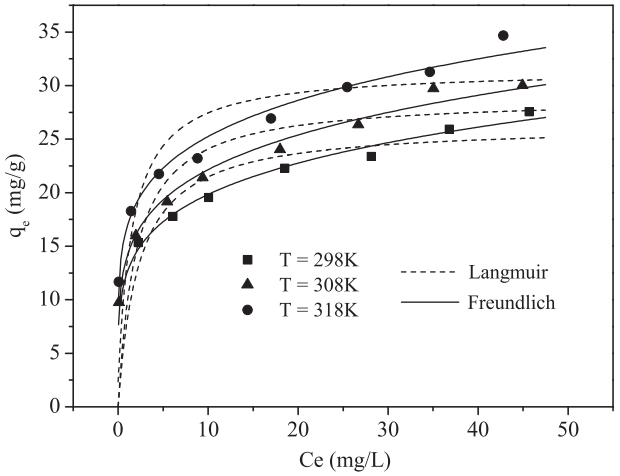


**Fig. 5.** Adsorption isotherms of P onto CMOMO at various temperatures. Symbols indicate experimental data; dash lines represent the Langmuir model; solid lines refer to the Freundlich model (experimental conditions: adsorbent dosage = 0.5 g/L, pH = 6.0 ± 0.1, equilibrium time = 24 h, $T$ = 298 K, 308 and 318 K).

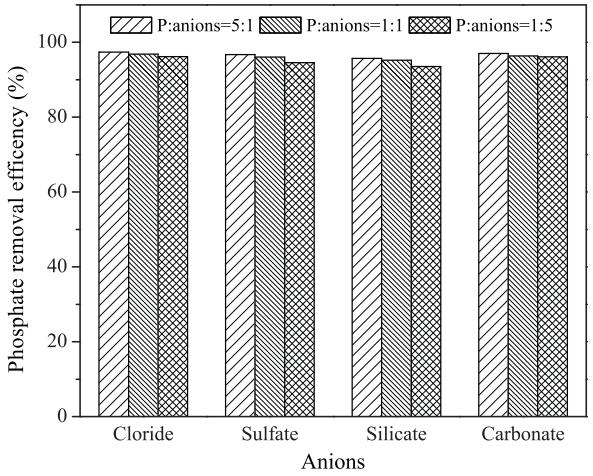


**Fig. 7.** Effects of coexisting anions on phosphate removal by CMOMO (experimental conditions: at fixed initial phosphate concentration = 5 mg/L, adsorbent dose = 0.5 g/L, pH = 6.0 ± 0.1, agitation speed = 130 rpm, $T$ = 298 K, equilibrium time = 24 h).

**Table 2**
Comparison of maximum phosphate adsorption capacity ($q_m$) of CMOMO with some other low-cost materials.

| Materials | $q_m$ (mg/g) | pH | References |
|---|---|---|---|
| CMOMO | 26.3 | 6 | Present study |
| Acid mine drainage sludge | 32.0 | 7 | [14] |
| Iron oxide tailings | 8.2 | 6.6 | [38] |
| Ferric sludge | 25.5 | 5.5 | [39] |
| Aluminum-based water treatment residual | 23.0 | 7 | [40] |
| Blast furnace slag | 18.9 | 7 | [41] |
| Fly ash | 20.2 | 9 | [42] |

negative $\Delta G$ values and positive $\Delta S$ value (70.3 J/mol K) indicated the spontaneous nature of the adsorption process. The positive $\Delta H$ value (5.32 kJ/mol) confirmed that the P adsorption in our study is an endothermic process.

### 3.4. Effects of pH and coexisting anions

Fig. 6 demonstrates the effects of solution pH and ion strength on the P adsorption by CMOMO. It can be seen that the P adsorption efficiency decreased with a solution pH increase, and the trend was similar with some other adsorbents used for P removal [14,43]. It

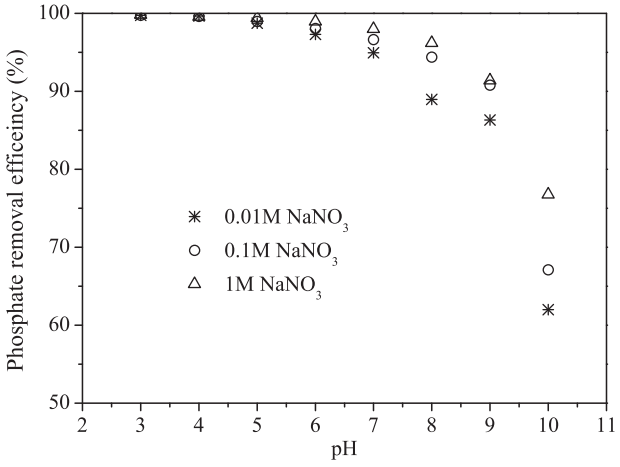


**Fig. 6.** Effects of pH and ion strength on the adsorption of P by CMOMO (experimental conditions: initial P = 5 mg/L, adsorbent dosage = 0.5 g/L, equilibrium time = 24 h).

was found by Nemeth et al. [44] that P adsorption on adsorbents is determined by the surface charge and the protonation state of P in the bulk solution. At the pH range of 2–10, the P species are mainly $HPO_4^{2-}$ and $H_2PO_4^-$ [45]. The iso-electric point ($pH_{IEP}$) of virgin CMOMO was 5.4 (Fig. S2), so the hydrated surface of CMOMO was protonated at pH > 5.4, exhibiting a net negative charge. Thus, the electrostatic repulsion between negatively charged adsorbents and P anions came into play and increased with the pH increase. In addition, the inhibition of P adsorption could also be ascribed to the competition between hydroxyl ions ($OH^-$) and the phosphate ions on the adsorbent surface [46]. The adsorption of P anions on the negatively charged surface of CMOMO under higher pH conditions was proposed to be driven mainly by specific adsorptions [47] and might depend on the initial concentrations of P in the solution. A shift to lower $pH_{IEP}$ of CMOMO after P adsorption (Fig. S2) consolidated that a specific adsorption rather other a pure electric interaction played an important role in the P adsorption.

On the other hand, P adsorption exhibited little ionic strength dependence below pH 5, whereas the P removal efficiency increased with an ion strength increase above pH 5. Inner-sphere complex is a complex-formation where ligands replace water molecules from the inner coordination sphere, and form bonds directly to the metal ion. In contrast, outer-sphere complex is another complex-formation in which the ligand is situated with no bonds forming directly to the metal ion [24]. It was founded [48] that ions forming inner-sphere complexes show an increase or no variation in the adsorption capacity with increasing ionic strength. In contrast, ions forming outer-sphere surface complexes exhibit decreasing the adsorption capacity with increasing solution ionic strength, which was formed mainly by electrostatic interactions and contain more than one water molecule between the adsorbate and the adsorbent functional groups. Therefore, the results suggested the inner-sphere mechanism was mainly involved in the process of P adsorption in our study.

Coexisting anions are generally present in the wastewater, which could interfere in the uptake of phosphate by adsorbent through competitive adsorption. Fig. 7 presents the effects of chloride ion, sulfate, silicate, and carbonate on the removal phosphate by CMOMO. It is shown that these anions have no significant influence on the phosphate adsorption. With the molar ratio of phosphate/silicate decreasing from 5:1 to 1:5, the P removal efficiency only decreased from 95.7% to 93.5%. The interferences of the other anions were even smaller. The results were in accordance

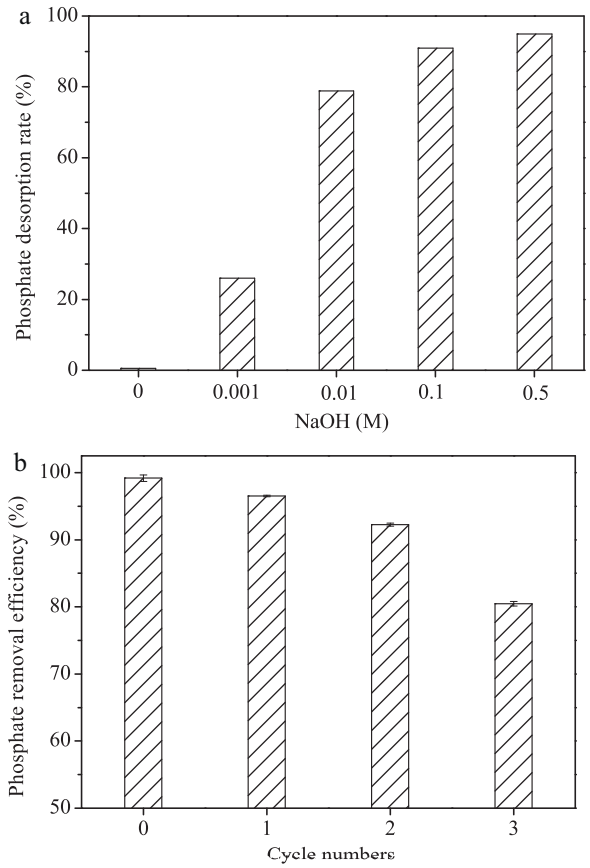


**Fig. 8.** Efficiency of (a) phosphate desorption from P-loaded CMOMO using different concentrations of NaOH solution (experimental conditions: adsorbent dose = 0.5 g/L, agitation speed = 130 rpm, $T$ = 298 K, equilibrium time = 24 h), and (b) phosphate adsorption using reused CMOMO in three consecutive cycles (experimental conditions: at fixed initial phosphate concentration = 5 mg/L, adsorbent dose = 0.5 g/L, agitation speed = 130 rpm, $T$ = 298 K, pH = 6.0 ± 0.1, equilibrium time = 24 h).

with the previous study of Zhang et al. [43], who found the negligible effects of coexisting anions on the phosphate removal by Fe–Mn binary oxide (FMBO) and attributed it to the high adsorption selectivity of FMBO. Thus, in our study, it is inferred that the adsorption of P was performed mainly through the mechanism of specific adsorption rather than that of ion exchange.

### 3.5. Desorption and regeneration

In the present study, different concentrations of NaOH solution were used to investigate the desorption process of the phosphate-loaded CMOMO. It is clearly presented in Fig. 8 that the amounts of phosphate desorption increased with the increase of alkalinity. The phosphate desorption percentages were determined to be 0.05%, 26.03%, 78.87%, 90.78% and 94.97%, when the concentrations of NaOH solution were 0 M, 0.001 M, 0.01 M, 0.1 M and 0.5 M, respectively. A desorption of only 0.6% was obtained when the extracting solution was 0.01 M $NaNO_3$ solution without NaOH adding. However, more than 93% of adsorbed phosphate was desorbed into the solution when the concentration of NaOH increased to 0.1 M. The further increase in the NaOH concentration (up to 0.5 M) did not significantly enhance the desorption of phosphate. It is indicated that the bonding between the active sites and the adsorbed phosphate was breakable, and the phosphate anions adsorbed onto CMOMO could be exchanged by $OH^-$ at high pH conditions. That is to say, CMOMO has a potential to be used as a renewable adsorbent. In order to testify the regeneration method of CMOMO, 3 cycles of consecutive regenerations were performed using 0.1 M NaOH as the eluent. Fig. 8b shows that at initial P = 5 mg/L, the P removal efficiency decreased from 99.2% to 96.5%, 92.2% and 80.4% after three regeneration cycles, respectively. There was an obvious decrease of P removal after the third regeneration. The adsorption loss might be due to the extraction of effective constituents (Al oxides) in CMOMO and the incomplete P desorption using alkali solutions as an eluent, especially for inner P complexes [49]. Nevertheless, the regenerated CMOMO was still cost-effective for P removal and the adsorbent can be used repeatedly at least for twice.

In the further study, pelletizing or coating methods will be used for the granulation of this adsorbent, which will be employed in dynamic column experiments for removing P from practical wastewater.

## 4. Conclusions

A new adsorbent was synthesized from manganese ore tailings for P removal using the process of digestion–oxidation–coprecipitation. It had an amorphous structure and a large BET area of 307.21 $m^2/g$, with the $pH_{IEP}$ value of 5.4. The kinetics data for P adsorption were best fitted by Elovich model due to the complicate composites of CMOMO. The maximum adsorption capacity for phosphate increased with an increase of temperature. Additionally, phosphate removal efficiency decreased with an increase of pH (4–10) or a decrease of ion strength (1–0.01 M). The marginal effects of the coexisting anions on phosphate removal suggested the specific adsorption of P by CMOMO. Furthermore, the P adsorption by CMOMO was reversible using NaOH solution as an eluent.

## Acknowledgements

This work was supported by the financial supports from Chinese Universities Scientific Fund (Grant No. QN2009037) and the Natural Science Foundation of China (Grant No. 51108377).

## Appendix A. Supplementary data

Supplementary data associated with this article can be found, in the online version, at doi:10.1016/j.jhazmat.2012.01.019.

## References

[1] D.J. Conley, H.W. Paerl, R.W. Howarth, D.F. Boesch, S.P. Seitzinger, K.E. Havens, C. Lancelot, G.E. Likens, Controlling eutrophication: nitrogen and phosphorus, Science 323 (20) (2009) 1014–1015.
[2] T. Clark, T. Stephenson, P.A. Pearce, Phosphorus removal by chemical precipitation in a biological aerated filter, Water Res. 31 (10) (1997) 2557–2563.
[3] S. Tsuneda, T. Ohno, K. Soejima, A. Hirata, Simultaneous nitrogen and phosphorus removal using denitrifying phosphate-accumulating organisms in a sequencing batch reactor, Biochem. Eng. J. 27 (3) (2006) 191–196.
[4] Y. Comeau, K.J. Hall, R.E.W. Hancock, W.K. Oldham, Biochemical model for enhanced biological phosphorus removal, Water Res. 20 (12) (1986) 1511–1521.
[5] S.L. Tian, P.R. Jiang, P. Ning, Y.H Su, Enhanced adsorption removal of phosphate from water by mixed lanthanum/aluminum pillared montmorillonite, Chem. Eng. J. 151 (1–3) (2009) 141–148.
[6] L.M. Blaney, S. Ginar, A.S. Gupta, Hybrid anion exchanger for trace phosphate removal from water and wastewater, Water Res. 41 (7) (2007) 1603–1613.
[7] Z. Geng, E.K. Hall, P.R. Berube, Membrane fouling mechanisms of a membrane enhanced biological phosphorus removal process, J. Membr. Sci. 296 (1–2) (2007) 93–101.
[8] N. Karapınar, Application of natural zeolite for phosphorus and ammonium removal from aqueous solutions, J. Hazard. Mater. 170 (2–3) (2009) 1186–1191.
[9] M. Khadhraoui, T. Watanabe, M. Kuroda, The effect of the physical structure of a porous Ca-based sorbent on its phosphorus removal capacity, Water Res. 36 (15) (2002) 3711–3718.
[10] J.A. Rentz, I.P. Turner, J.L. Ullman, Removal of phosphorus from solution using biogenic iron oxides, Water Res. 43 (7) (2009) 2009–2035.
[11] N. Kawasaki, F. Ogata, H. Tominaga, Selective adsorption behavior of phosphate onto aluminum hydroxide gel, J. Hazard. Mater. 181 (1–3) (2010) 574–579.

[12] A. Bhatnagar, M. Sillanpää, Utilization of agro-industrial and municipal waste materials as potential adsorbents for water treatment—a review, Chem. Eng. J. 157 (2–3) (2010) 277–296.
[13] A.O. Babatunde, Y.Q. Zhao, A.M. Burke, M.A. Morris, J.P. Hanrahan, Characterization of aluminium-based water treatment residual for potential phosphorus removal in engineered wetlands, Environ. Pollut. 157 (2009) 2830–2836.
[14] X. Wei, R.C. Viadero Jr., S. Bhojappa, Phosphorus removal by acid mine drainage sludge from secondary effluents of municipal wastewater treatment plants, Water Res. 42 (13) (2008) 3275–3284.
[15] G. Gong, S. Ye, Y. Tian, Q. Wang, J. Ni, Y. Chen, Preparation of a new sorbent with hydrated lime and blast furnace slag for phosphorus removal from aqueous solution, J. Hazard. Mater. 166 (2–3) (2009) 714–719.
[16] P.L. Sibrella, G.A. Montgomerya, K.L. Ritenoura, T.W. Tuckerb, Removal of phosphorus from agricultural wastewaters using adsorption media prepared from acid mine drainage sludge, Water Res. 43 (8) (2009) 2240–2250.
[17] J. Routh, M. Ikramuddin, Trace-element geochemistry of Onion Creek near Van Stone lead–zinc mine (Washington, USA) chemical analysis and geochemical modeling, Chem. Geol. 133 (1–4) (1996) 211–224.
[18] C. Roussel, H. Bril, A. Fernandez, Arsenic speciation: involvement in evaluation of environmental impact caused by mine wastes, J. Environ. Qual. 29 (1) (2000) 182–188.
[19] K. Wu, R. Liu, H. Liu, X. Zhao, J. Qu, Arsenic(III,V) adsorption on iron-oxide-coated manganese sand and quartz sand: comparison of different carriers and adsorption capacities, Environ. Eng. Sci. 28 (9) (2011) 643–651.
[20] Y. Darmane, M. Cherkaoui, S. Kitane, A. Alaoui, A. Sebban, M. Ebn Touhami, Preparation of chemical manganese dioxide from Moroccan pyrolusite mine waste, Hydrometallurgy 92 (1–2) (2008) 73–78.
[21] Z.Y. Hseu, Z.S. Chen, C.C. Tsai, C.C. Tsui, S.F. Cheng, C.L. Liu, H.T. Lin, Digestion methods for total heavy metals in sediments and soils, Water Air Soil Pollut. 141 (1–4) (2002) 189–205.
[22] Y.S. Ho, G. Mckay, Sorption of dye from aqueous solution by peat, Chem. Eng. J. 70 (1998) 115–124.
[23] Y.S. Ho, G. Mckay, Kinetic models for the sorption of dye from aqueous solution by wood, J. Environ. Sci. Health Part B: Process Saf. Environ. Prot. 76 (B) (1998) 184–185.
[24] D.L. Sparks, Kinetics of Soil Chemical Processes, Academic Press, New York, 1989.
[25] W.J. Weber Jr., J.C. Morris, Kinetics of adsorption on carbon from solution, J. Sanitary Eng. Div. 89 (2) (1963) 31–60.
[26] I. Langmuir, The adsorption of gases on plane surfaces of glass, mica and platinum, J. Am. Chem. Soc. 40 (1918) 1361–1403.
[27] H.M.F. Freudlich, Ünber die adsorption in lösungen, Z. Phys. Chem. (Leipzig) 57 (A) (1906) 385–470.
[28] M. Doula, A. Ioannou, A. Dimirkou, Thermodynamics of copper adsorption–desorption by Ca-kaolinite, Adsorption 6 (4) (2000) 325–335.
[29] L.T. Chiem, L. Huynh, J. Ralston, D.A. Beattie, An in situ ATR–FTIR study of polyacrylamide adsorption at the talc surface, J. Colloid Interface Sci. 297 (1) (2006) 54–61.
[30] V. Lenoble, C. Laclautre, B. Serpaud, V. Deluchat, J.C. Bollinger, As(V) retention and As(III) simultaneous oxidation and removal on a $MnO_2$-loaded polystyrene resin, Sci. Total Environ. 326 (1–3) (2004) 197–207.
[31] J.F. Moulder, W.F. Stickle, P.E. Sobol, K.D. Bomben, Handbook of X-ray Photoelectron Spectroscopy, Perkin-Elmer, Norwalk, 1992.
[32] H.W. Nesbitt, G.W. Canning, G.M. Bancroft, XPS study of reductive dissolution of 7 Å-birnessite by $H_3AsO_3$ with constraints on reaction mechanism, Geochim. Cosmochim. Acta 62 (12) (1998) 2097–2110.
[33] F. Arias, T.K. Sen, Removal of zinc metal ion ($Zn^{2+}$) from its aqueous solution by kaolin clay mineral: a kinetic and equilibrium study, Colloids Surf. A348 (1–3) (2009) 100–108.
[34] T.K. Sen, M.V. Sarzali, Removal of cadmium metal ion ($Cd^{2+}$) from its aqueous solution by aluminum oxide ($Al_2O_3$): a kinetic and equilibrium study, Chem. Eng. J. 142 (3) (2008) 256–262.
[35] J.S. Geelhoed, T. Hiemstra, W.H.V. Riemsdijk, Phosphate and sulfate adsorption on goethite: single anion and competitive adsorption, Geochim. Cosmochim. Acta 61 (12) (1997) 2389–2396.
[36] W. Rudzinski, W.A. Steele, G. Zgrablich, Equilibria and Dynamics of Gas Adsorption on Heterogeneous Solid Surfaces, Elsevier, Amsterdam, 1996, p. 202.
[37] S.H. Chien, W.R. Clayton, Application of Elovich equation to the kinetics of phosphate release and sorption in soils, Soil Sci. Soc. Am. J. 44 (1980) 265–268.
[38] L. Zeng, X. Li, J. Liu, Adsorptive removal of phosphate from aqueous solutions using iron oxide tailings, Water Res. 38 (5) (2004) 1318–1326.
[39] X. Song, Y. Pan, Q. Wu, Z. Cheng, W. Ma, Phosphate removal from aqueous solutions by adsorption using ferric sludge, Desalination 280 (2011) 384–390.
[40] A.O. Babatunde, Y. Zhao, A.M. Burke, M.A. Morris, J.P. Hanrahan, Characterization of aluminium-based water treatment residual for potential phosphorus removal in engineered wetlands, Environ. Pollut. 157 (2009) 2830–2836.
[41] B. Kostura, H. Kulveitová, J. Leško, Blast furnace slags as sorbents of phosphate from water solutions, Water Res. 39 (2005) 1795–1802.
[42] J. Chen, H. Kong, D. Wu, X. Chen, D. Zhang, Z. Sun, Phosphate immobilization from aqueous solution by fly ashes in relation to their composition, J. Hazard. Mater. 139 (2007) 293–300.
[43] G. Zhang, H. Liu, R. Liu, J. Qu, Removal of phosphate from water by a Fe–Mn binary oxide adsorbent, J. Colloid Interface Sci. 335 (2) (2009) 168–174.
[44] Z. Nemeth, G. Gancs, G. Gemes, A. Kolics, pH dependence of phosphate sorption on aluminum, Corros. Sci. 40 (2) (1998) 2023–2027.
[45] A. Ringbom, Complexation in Analytical Chemistry, Interscience Publishers, New York/London, 1963.
[46] H. Liu, X. Sun, C. Yin, C. Hu, Removal of phosphate by mesoporous $ZrO_2$, J. Hazard. Mater. 151 (2–3) (2008) 616–622.
[47] A.B. Pérez-Marín, V.M. Zapata, J.F. Ortuno, M. Aguilar, J. Sàez, M. Lloréns, Removal of cadmium from aqueous solutions by adsorption onto orangewaste, J. Hazard. Mater. 139 (1) (2007) 122–131.
[48] G. Sposito, The Surface Chemistry of Soils, Oxford University Press, Oxford, England, 1984.
[49] A.Z. Maor, R. Semiat, H. Shemer, Adsorption–desorption mechanism of phosphate by immobilized nano-sized magnetite layer: interface and bulk interactions, J. Colloid Interface Sci. 363 (2011) 608–614.